Volume 1 Number 1 ISSN: 1551–1286 (Print) ISSN: 1551–1294 (Online)

NanoBiotechnology

The Journal at the Intersection of Nanotechnology, Molecular Biology, and Biomedical Sciences

HUMANA PRESS

NanoBiotechnology

ISSN 1551-1286/05/01:113–120/$30.00
DOI: 10.1385/Nano:1:1:113

Original Article

Near-Field Fluorescence Microscopy

An Optical Nanotool to Study Protein Organization at the Cell Membrane

María F. García-Parajó,[1] Bärbel I. de Bakker,[1] Marjolein Koopman,[1] Alessandra Cambi,[2] Frank de Lange,[2] Carl G. Figdor,[2] and Niek F. van Hulst[1]

[1]Applied Optics Group, Faculty of Science & Technology, MESA† Institute for Nanotechnology, University of Twente, The Netherlands; [2]Department of Tumor Immunology, Nijmegen Center for Molecular Life Sciences, University Medical Center, Nijmegen, The Netherlands

Abstract

The ability to study the structure and function of cell membranes and membrane components is fundamental to understanding cellular processes. This requires the use of methods capable of resolving structures with nanometer-scale resolution in intact or living cells. Although fluorescence microscopy has proven to be an extremely versatile tool in cell biology, its diffraction-limited resolution prevents the investigation of membrane compartmentalization at the nanometer scale. Near-field scanning optical microscopy (NSOM) is a relatively unexplored technique that combines both enhanced spatial resolution of probing microscopes and simultaneous measurement of topographic and optical signals. Because of the very small near-field excitation volume, background fluorescence from the cytoplasm is effectively reduced, enabling the visualization of nano-scale domains on the cell membrane with single molecule detection sensitivity at physiologically relevant packing densities. In this article we discuss technological aspects concerning the implementation of NSOM for cell membrane studies and illustrate its unique advantages in terms of spatial resolution, background suppression, sensitivity, and surface specificity for the study of protein clustering at the cell membrane. Furthermore, we demonstrate reliable operation under physiological conditions, without compromising resolution or sensitivity, opening the road toward truly live cell imaging with unprecedented detail and accuracy.

(Nanobiotechnology DOI: 10.1385/Nano:1:1:113)

Key Words: Near-field scanning optical microscopy (NSOM); single molecule detection (SMD); cell membrane compartmentalization; high-resolution optical microscopy.

Correspondence and reprint requests to:

María F. García-Parajó, Applied Optics Group, Faculty of Science and Technology, MESA† Institute for Nanotechnology, University of Twente, P.O. Box 217, 7500 AE Enschede, The Netherlands.
E-mail: M.F.Garciaparajo@tn.utwente.nl

Humana Press

Introduction

One of the most fascinating but also controversial fields in cell biology concerns the organization of the cellular plasma membrane. In fact, the view of the cell membrane as a two-dimensional homogeneous structure has changed radically in recent years by demonstrations of lateral heterogeneities, patches, and the existence of protein domains in the membrane *(1–3)*. The general consensus points to a direct relation between the lateral organization of proteins and lipids and their specific cellular function *(4–7)*. Similarly, a large body of evidence indicates that the size of many of these membrane domains is in the range of 30–800 nm *(6,8)*. Part of the controversy regarding the existence of membrane domains lies in their physical size, being smaller than the diffraction limit of light, and thus not resolvable by optical means. Moreover, there is increasing evidence that the assembly and disassembly of such complexes is a rather dynamic process *(6)*. Finally, biochemical and biophysical approaches aimed at the study of protein domains have lead in many cases to

contradictory results *(9,10)*. There is therefore need for new high-resolution methodologies capable of directly imaging domains within the plasma membrane of intact cells.

Fluorescence microscopy has become one of the most prominent and versatile research tools used in modern cell biology (*11*, and references therein). The reasons for it are essentially twofold. On the one hand, light-based microscopy allows the study of living specimens in their native environment in a noninvasive manner. Additionally, fluorescence microscopy offers chemical specificity by exploiting polarization, lifetime, and spectral contrast *(12)*. Furthermore, progress in detector technology has recently pushed fluorescence microscopy to its ultimate level of sensitivity: the detection of individual molecules *(13–15)*. On the other hand, enormous progress on the development of specific and highly efficient fluorescent probes for exogenous labeling has been achieved. In parallel to external antibody labeling, the advent of green fluorescent protein (GFP) technology has revolutionized live cell imaging because an autofluorescent molecule can be genetically encoded as a fusion with the c-DNA of interest *(16)*. The spectral variants of GFP and the unrelated red fluorescent protein (DsRed) make it possible to perform multicolor imaging in living cells *(16,17)*.

In the last few years, a number of optical-based techniques have been applied to study the organization of the cellular plasma membrane. Figure 1 illustrates some of the most commonly used approaches. In total internal reflection microscopy (Fig. 1A) an evanescent field is created at the interface between the glass substrate and the cell surface. Because the excitation intensity decays exponentially as a function of the distance from the glass–cell interface, it allows selective excitation at the cell membrane. The technique is widely used for single molecule detection both in vitro and in vivo and has the capability of monitoring dynamic processes with high time resolution (*18*, and references therein). Unfortunately, only the membrane–glass interface is effectively illuminated, a region where, most probably, dynamical processes are hindered by the presence of the glass substrate. Furthermore, the lateral resolution in such a methodology is limited to length scales > 300 nm, lacking the spatial resolution necessary to probe nano-scale organization of membrane components. In scanning confocal microscopy (Fig. 1B) the detection volume is reduced by using a pinhole that rejects out-of-focus light and enables imaging of thin sections of the cell, in particular the cell membrane. Nevertheless, the lateral resolution is still diffraction-limited and, because the penetration depth in the axial direction is on the order of the wavelength used, background from cellular autofluorescent components is a problem for single molecule detection. Recently, 4Pi and stimulated-emission depletion microscopy have been developed with the aim of improving the lateral resolution of confocal microscopy *(19,20)*. Both techniques have demonstrated increased lateral and axial resolution *(19,20)*, although broad applicability still needs to be shown convincingly. A successful and broadly applied method to gain contrast at the nanometer scale is fluorescence resonance energy transfer (FRET) (*21*, and references therein). The efficiency of the energy transfer process is strongly dependent on the fluorophores distance separation (r^{-6}) and thus ideally suited to investigate proximity and interactions between proteins in the 1–10 nm spatial scale *(9,21)*. Thus, while diffraction-limited methods are able to visualize structures larger than 300 nm, FRET focuses on processes occurring at distances smaller than 10 nm, leaving behind a considerable and important spatial gap inaccessible to optical investigation.

Near-field scanning optical microscopy (NSOM) is a promising optical technique able to bridge this gap by bringing spatial resolution down to the level of several tens of nanometers. This contribution focuses on the application of NSOM to investigate, with single molecule detection sensitivity, the lateral organization of the cell membrane in intact cells with a spatial resolution better than 100 nm. Our results clearly show the suppression of autofluorescence background when imaging the cell membrane, facilitating the visualization of nano-scale protein domains. Furthermore, we discuss the added value of combining single molecule detection sensitivity with high spatial resolution for discriminating monomer vs clustered organization. Finally, we demonstrate that NSOM is capable of routine liquid operation enabling the study of the cell membrane in native conditions, opening new ways to investigate the relation between membrane organization and cell function.

Near-Field Scanning Optical Microscopy (NSOM)

NSOM is a technique that preserves the advantages of the evanescent type of illumination, while simultaneously providing lateral resolution beyond the diffraction limit of light. The technique (*see* Fig. 1C) is based on scanning a small subwavelength aperture probe in close proximity to the sample surface. The lateral resolution, down to tens of nanometers, is essentially defined by the size of the aperture and the sample-to-probe distance. The probe illuminates the sample with an evanescent field that is strongly localized at the vicinity of the aperture and decreases very rapidly away from the probe's end face *(22,23)*. Owing to the exponentially decaying character of the illumination field, NSOM is a surface-sensitive technique, and it is therefore ideal for studying the cell membrane *(24,25)*. In addition to its surface sensitivity, NSOM provides simultaneous topographic and fluorescence imaging *(22–24,26)*. Finally, the small excitation volume (10^5 nm^3 vs 10^8 nm^3 as obtained in confocal microscopy) reduces dramatically the cytoplasm background fluorescence, enabling single molecule detection on the cell membrane *(24)* with a high signal-to-background ratio.

Despite its apparent advantages, the application of NSOM to biology has witnessed only modest progress. Successful examples on cell membrane studies include the co-localization of proteins within the membrane of malaria parasite-infected red blood cells at a resolution of approx 100 nm *(27)*, mapping the clustering of major histocompatibility complexes I and II in fibroblast cells *(28)*, identification of membrane lipid

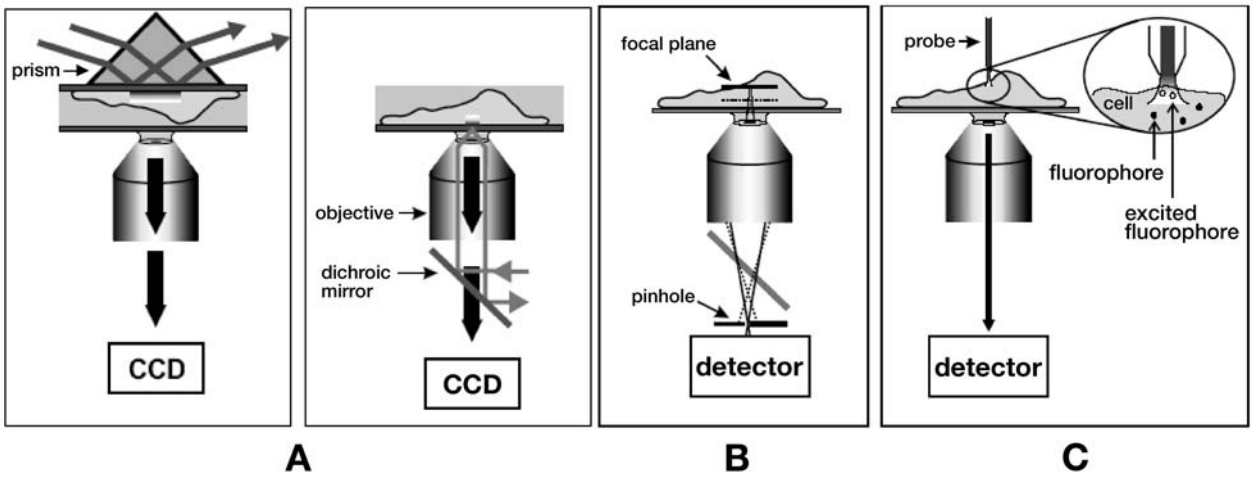

Fig. 1. Schematics of the different experimental schemes to investigate the organization of the cellular plasma membrane. **(A)** Total internal reflection microscopy relies on the generation of an evanescent field at the interface between glass (high-refractive-index material) and the cell surface (low-refractive-index material). The evanescent field penetrates into the medium of lower refractive index and decreases exponentially with the distance from the interface. Two practical configurations are normally used to generate the evanescent field, i.e., via a prism or using the edges of a high NA objective. The objective collects the fluorescence, which is filtered from the excitation light and detected by a two-dimensional array detector, normally a CCD camera. **(B)** In confocal microscopy the excitation light is collimated, reflected by a dichroic mirror, and focused onto the sample (path not shown). Fluorescence from the focal plane (solid line) and from out-of-focus regions (dotted line) are collected by the same objective, filtered, and detected by an avalanche photodiode (APD). Out-of-focus light is rejected by using a pinhole in front of the detector. **(C)** In near-field scanning optical microscopy a subwavelength aperture probe illuminates the upper part of the cell membrane. Fluorescence is collected in the far-field using a high NA objective, filtered, and detected with an APD.

and proteins on fibroblast *(29)*, and the study of ion channel clusters in cardiac myocyte membranes *(30)*. More recently, we have used the technique to investigate the nano-scale organization of C-type lectins on the membrane of immature dendritic cells, both under dry and liquid conditions *(31,32)*.

Figure 2A shows the schematics of the combined confocal/NSOM microscope routinely used in our experiments. The experimental set-up is integrated into an inverted optical microscope (Zeiss Axiovert 135TV). The microscope has access to two Ar^+/Kr^+ ion lasers, providing a wide wavelength range (457–647 nm). Laser light enters the set-up via two optical paths where adjustment of the beam width, excitation intensity, and polarization are controlled independently. Both beams are then combined by a beam splitter (not shown). In confocal mode, the light is guided through a short piece of single mode fiber that acts as a spatial filter, guaranteeing full overlay of the two wavelengths. After a beam expander, the incoming circularly polarized light is reflected by a dichroic mirror and focused onto the sample using an oil-immersion objective (Olympus, ×64, 1.4 NA). In the NSOM mode, single or dual excitation light is coupled into an Al-coated tapered fiber probe (single mode, $\lambda = 633$ nm, Cunz, Frankfurt). A flipable mirror mount (Newfocus Inc.) enables easy switching between confocal and NSOM excitation modes. On the detection side, the emitted fluorescence is collected by the objective and selected using appropriate long-pass filters. The fluorescence is then separated in two channels, with either polarization or spectral contrast, and focused onto two avalanche photodiodes (SPCM-100, EG&G, Quebec).

One of the crucial aspects of NSOM relies on the fabrication of reproducible aperture probes. Our probes are based on single-mode optical fibers, fabricated using the "heating and pulling" method, followed by an Al deposition layer (approx 100 nm) in order to confine the light within the probe (*see* Fig. 2B) *(33)*. Typical sizes are 70–100 nm with throughput efficiency of 10^{-5}–10^{-4}, depending on the aperture size *(33)*. The probe is kept in the near-field region of the sample (<10 nm) by means of a shear-force feedback based on a piezoelectric element, providing simultaneously a topographic map of the sample surface while scanning *(23,24,26)*. Recently, we have developed a reliable and easy-to-use system, with perfect analogy to a diving bell, to allow NSOM operation under liquid conditions *(34)*. A small glass tube, carefully glued into an aluminum holder, as shown in Fig. 2C, encapsulates the piezoelectric element, so that vibration is performed in air. A small part of the NSOM probe protrudes out of the glass tube and is in contact with the wet sample. Using this concept we have shown that NSOM is able to operate in liquid environments without compromising resolution or sensitivity *(32)*.

High-Resolution Single Molecule Imaging Using NSOM

To demonstrate the potential of NSOM as a high-resolution optical technique to study the organization of proteins on the cell membrane, we have investigated the distribution of the C-type lectin DC-SIGN expressed on dendritic cells (DC). Figure 3A shows a bright-field image of an adherent DC on a glass substrate, while Fig. 3B,D show fluorescence

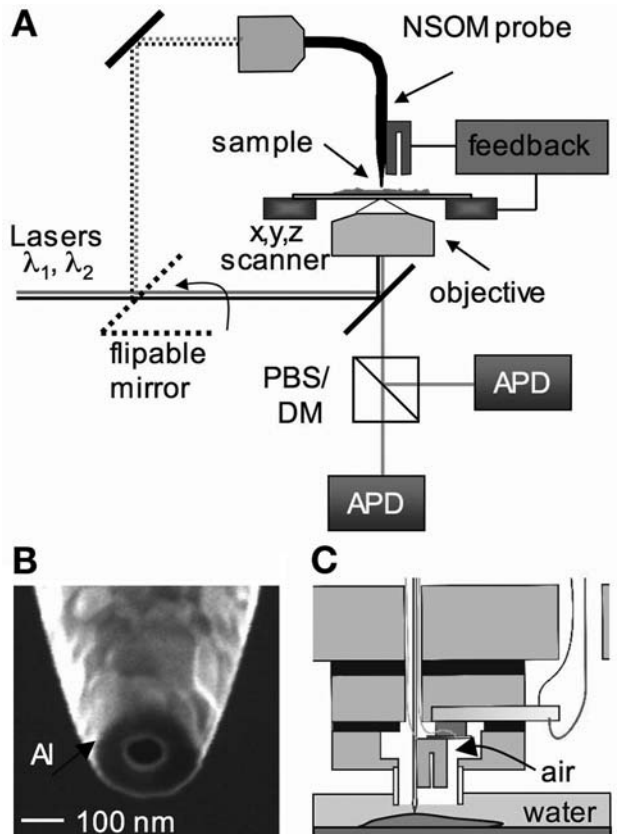

Fig. 2. (A) Schematics layout of the combined confocal/NSOM set-up. Two laser lines can be simultaneously coupled into the microscope using the confocal or NSOM excitation configuration modes. Fluorescence light is collected using a high NA objective and selected using appropriate filters. The fluorescence signal is then separated according its polarization [using a polarizing beam splitter (PBS)] or spectral [using a dichroic mirror (DM)] properties and sent to two APDs. **(B)** Focused ion beam image of a 70 nm diameter NSOM probe. The aperture functions as a local light source, and its diameter primarily determines the optical resolution of the microscope. Because of the evanescent character of the light exiting the probe, the optical near-field excitation has significant intensity only in a layer of <100 nm away from the aperture. This essentially means that lower-lying fluorophores are not excited, resulting in an effective suppression of background fluorescence. **(C)** Schematic drawing of the diving bell concept implemented for NSOM operation in liquid conditions. Only the tip end (approx 100 μm) is immersed in liquid, while the tuning-fork piezoelectric element is vibrating in air.

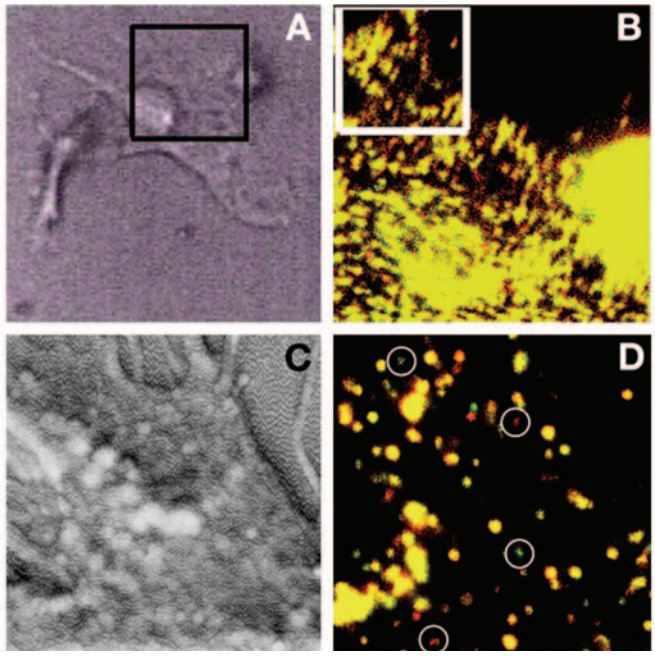

Fig. 3. DC-SIGN externally labeled with Cy5 on an immature DC. Cells were stretched on fibronectin-coated glass coverslips. Cells were incubated with primary monoclonal antibodies against DC-SIGN in PBA (10 mg/mL, 25 min). After two washing steps with PBA, a second incubation was performed with goat anti-mouse Cy5, 1:25 in PBA for 25 min. Samples were subsequently fixed with 1% paraformaldehyde in PBS, dehydrated, and critical-point dried. A selected area of interest in the bright field image of **(A)** is imaged in confocal mode (20 μm^2) **(B)**. The selected area in the confocal image was further investigated with NSOM. **(C)** Shear-force topographic image simultaneously obtained with the near-field fluorescence image (7 μm^2) **(D)**. In both **(B)** and **(D)** the fluorescence signal is color-coded according to the detected polarization, red for 0° and green for 90°. Some individual molecules are apparent in **(D)** and highlighted in circles to demonstrate the single molecule detection sensitivity of the set-up. Individual molecules are identified by their unique dipole emission, i.e., red and green color-coding. The yellow color of most fluorescent spots results from adding multiple molecules with random in-plane orientation (combination of red and green) in one spot.

measurements of DC-SIGN externally labeled via antibodies conjugated to the fluorophore Cy5. In both confocal (Fig. 3B) and NSOM (Fig. 3D), the brightness of the images reflect the number of proteins expressed on the membrane while the color is related to the polarization of fluorescence signal. Figure 3C shows the topography of the membrane obtained simultaneously while recording the near-field optical image.

The confocal image in Fig. 3B exhibits a large intensity spread over the cell surface. The smallest visible features are around 350 nm, close to the diffraction limit. The high fluorescence intensity results from the high expression level of DC-SIGN and a considerable contribution from cell auto-fluorescence (see also next section). From the confocal image it is hard to distinguish isolated components on the cell surface. In contrast to the confocal image, the high-resolution near-field image (Fig. 3D) reveals details within the fluorescent patches and clearly resolves separate spots on the membrane. As clearly observed in Fig. 3D, the fluorescence spots differ in brightness, size, and emission polarization. The presence of well-defined polarized emission (color of some spots being either green or red) is indicative of unique dipole emission and thus single molecule detection. However, the large majority of the spots have a yellow color, indicating emission from multiple dipoles, and thus protein clustering. Accordingly, the brightness and size of these spots are larger than those

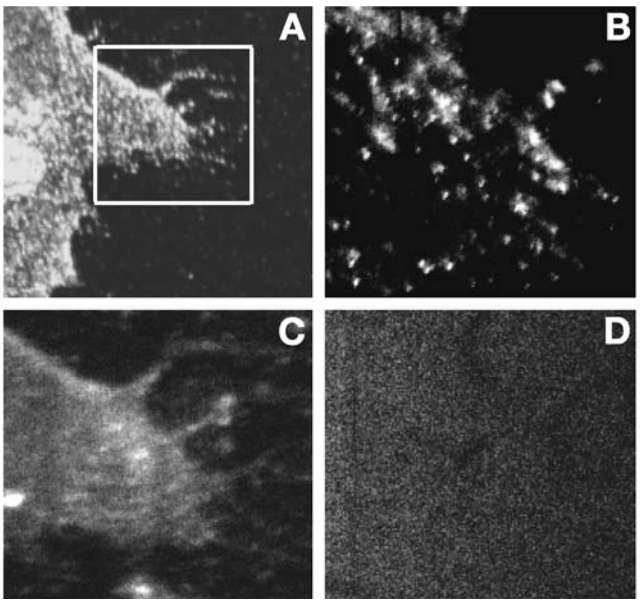

Fig. 4. (A) Confocal fluorescence image of a Cy5-labeled cell membrane excited with 647 nm excitation light, coinciding with the Cy5 peak in the absorption spectrum. **(B)** NSOM image of the highlighted region in **(A),** using the same excitation wavelength. **(C)** Confocal image of the highlighted area at an excitation wavelength of 514 nm, outside the absorption region of Cy5. The fluorescence contrast (40 kcounts/s on the cell surface vs 4.5 kcounts/s on the glass substrate) is due to autofluorescence background generated by intracellular components upon excitation at 514.5 nm. **(D)** NSOM image of the same area showing essentially no contrast between cell and glass substrate at 514.5 nm (3.6 kcounts/s). The excitation power in **(C)** and **(D)** is 2.7 kW/cm^2.

arising from single molecule emission. These findings confirm and extend our previous observations that DC-SIGN is not randomly distributed as individual molecules but rather is clustered in domains *(7)*. It also demonstrates that NSOM is equally capable [as compared to electron microscopy (EM)] to resolve the static heterogeneity of the cell membrane with high resolution. Moreover, as surface scanning technique, NSOM is able to follow the 3D cell topology (Fig. 3C) in contrast to EM which is exclusively a 2D technique. The cell height in the dendrite region varied from tens of nanometers to 250 nm as derived from the topographic image shown in Fig. 3C, confirming that the cell is well stretched on the substrate. Finally, the combination of topography and fluorescence intensity also allows the determination of the absolute position of the fluorescent spots on the membrane.

Background Reduction and Surface Specificity of NSOM

One of the major difficulties when discriminating individual molecules on the cell membrane is the large fluorescence background generated by intracellular components. The shallow penetration depth of the evanescent field emanating from the NSOM probe (<100 nm) greatly suppresses the autofluorescence from the cell. As a demonstration, Fig. 4 shows a DC expressing Cy5-labeled DC-SIGN and imaged in confocal (A) and NSOM (B) modes. In the upper figures, the sample is excited at a wavelength of 647 nm, matching the peak of Cy5 absorption. The advantage of NSOM in terms of spatial resolution is again clearly visible when comparing both images. Yet, even more striking is the large fluorescence background suppression obtained by NSOM. In the lower figures, an excitation wavelength of 514.5 nm, outside the absorption spectrum of Cy5, has been used. While the confocal image (C) exhibits large fluorescence contrast resulting from the excitation of the cytoplasm and contributing substantially to the increase of background signal, the NSOM image of the same region (D) is virtually free of background. No contrast between glass and the membrane is observed, thus demonstrating the surface specificity of the technique and the added value when investigating the cellular membrane.

Extracting Quantitative Information from NSOM Images

Although from a first inspection of the NSOM images a qualitative impression on the spatial organization of protein components on the cell membrane is readily obtained, more quantitative insight on their organization can be gained by analyzing the fluorescence spots in terms of their intensity, size, and relative position on the cell surface. Figure 5A shows as an example a typical near-field fluorescence image in 3D, highlighting the most important features of the fluorescence spots. The total number of detected photon counts from a spot is directly related to the number of fluorophores and thus to the number of proteins, depending on the antibody labeling efficiency. As observed from Fig. 5A the fluorescence varies from spot to spot, indicating a wide spread on the number of proteins involved in each spot. The single molecule detection sensitivity of our set-up allows us to build up intensity distributions of all fluorescent spots, thus deriving the relative number of proteins being monomeric vs clustered in domains. In the particular case of DC-SIGN, we have demonstrated recently that more than 80% of the proteins expressed on immature DCs are organized on domains, each cluster hosting from a few to several tens of DC-SIGN molecules *(31)*.

Further evidence for protein clustering is obtained by measuring the physical size of each fluorescent spot. The size is determined by fitting the measured intensity profile with a 2D Gaussian function. The spot size is then defined as the full-width at half-maximum (FWHM) of the fit. A histogram of spot sizes as obtained from imaging DC-SIGN using NSOM is shown in Fig. 5B. The spot sizes vary from 70 to 650 nm with a peak at 200 nm. The inset in Fig. 5B shows the FWHM of a single molecule fluorescent spot reflecting the size of the aperture probe, and being clearly below the peak of the distribution. Noticeably, the size of the clusters is below the diffraction limit of light and therefore not accessible by standard optical means. The high spatial resolution of NSOM is therefore crucial to directly resolve the physical size of

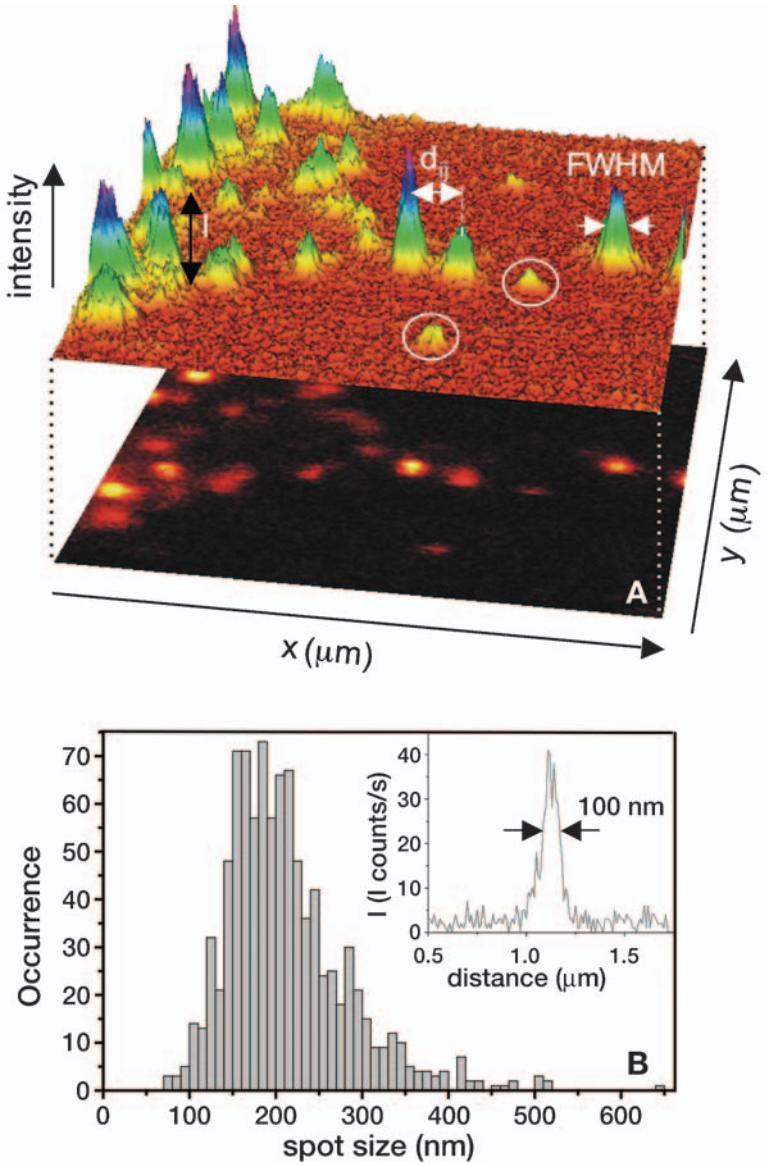

Fig. 5. (A) Information extracted from a typical NSOM image (3 μm^2, 256 x 256 pixels). The fluorescence in the upper image is plotted in 3D with *x* and *y* as spatial axes and a vertical intensity axis. The fluorescent spots differ in intensity *(I)* and size (FWHM). The circles point to single molecule spots. The spatial position of each spot is given by the center of coordinates of its intensity profile after fitting with a Gaussian function. The nearest-neighbor distance between two spots *i* and *j* is indicated by d_{ij}. **(B)** Spot size distribution (FWHM) of 1200 different measured spots. The intensity profile through a single molecule spot is shown in the inset of **(B)**.

nanometric-sized domains on the cell membrane without the need of de-convolution algorithms *(31)*.

A final parameter of interest when studying the distribution of protein components on the cell membrane concerns their relative position. Mutual spot distances can be easily examined by means of nearest-neighbor-distance (nnd) analysis, where the *(x,y)* position of each spot is determined from the peak position of a Gauss fit to the intensity profile. We have performed nnd analysis on the DC-SIGN images obtaining an intercluster distance distribution peaking approx 450 nm *(31)*. On the other hand, by making use of the single molecule photon counting histograms, we have determined an average content of 30 Cy5 molecules per domain, with a surface coverage of approx 2.5 domains/μm^2 *(31)*. In the case of a random distribution of proteins on the cell surface, the nnd is given by nnd = $1/(2\rho^{1/2})$, where ρ is the protein density on the cell surface. The mutual separation for individual molecules organized in a random fashion would then result in approx 60 nm, which is clearly smaller than obtained in our experiments. If, on the other hand, the molecules are bunched in clusters, a larger distance separation between clusters should be expected as compared to the random case. Our results are therefore a further proof of protein clustering in the cell membrane.

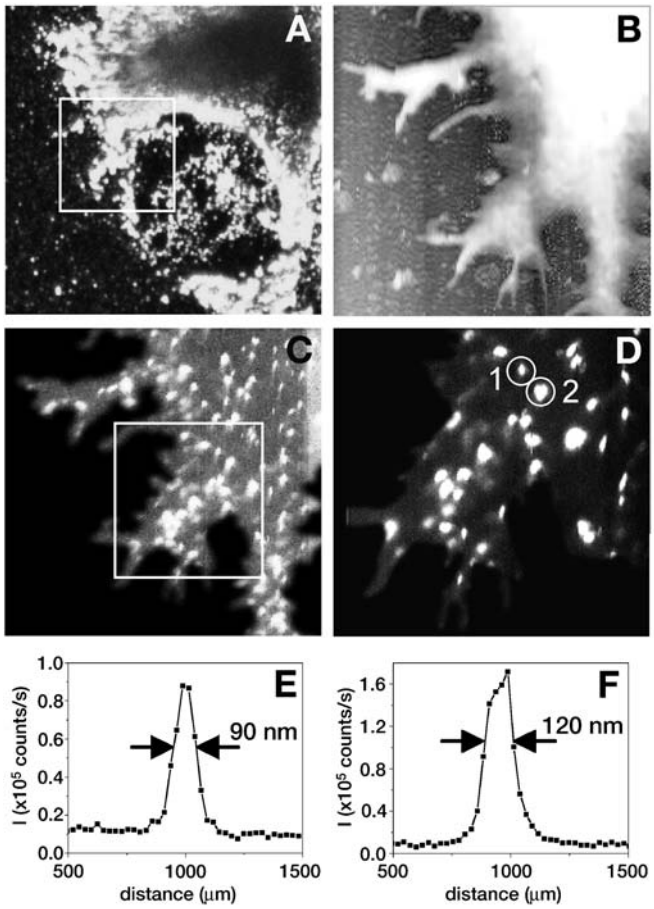

Fig. 6. (A) Fluorescence image of an immature dendritic cell in buffer solution collected in confocal mode (32 μm^2). Samples were prepared in a similar fashion as described in the text, but without the dehydration and critical point dry steps. Wet samples were stored in PBS containing 1% paraformaldehyde until use. Simultaneously obtained topography **(B)** and NSOM **(C)** image (16.5 μm^2) of the highlighted area in **(A)**. **(D)** Zoom-in NSOM image (7 μm^2) of the area highlighted in **(C)**. **(E)** and **(F)** show line traces along the two clusters encircled in **(D),** demonstrating the high spatial resolution of NSOM.

High-Resolution NSOM Imaging in Liquid

The most technical challenge associated with the use of NSOM for biological research concerns the difficulty of operating the technique in physiological relevant conditions. Although important biological information can be extracted from NSOM on dry biological samples, these results are always subject to potential drying artifacts *(35)*. We have recently shown that the performance of NSOM can be extended to measurements in liquid environments using a diving bell concept *(34)*, and showed for the first time single molecule detection sensitivity with 90 nm spatial resolution on wet cells *(32)*. To demonstrate the general applicability of NSOM for cell membrane studies in liquid conditions, we have extended our investigation of the organization of DC-SIGN to wet dendritic cells. Figure 6A shows the confocal image of a large region of a DC expressing DC-SIGN on the surface, while Figs. 6B and 6C show the simultaneously obtained topographic and near-field image of a highlighted region of the membrane. As clearly observed from the NSOM image, operation in liquid is successfully achieved with similar sensitivity and resolution as obtained on dried material (Fig. 3). The topographic image in Fig. 6B serves as a mask to identify the contours and the cell region, excluding any possible fluorescence misassignment due to unspecific binding of antibodies to the glass substrate. A further zoom-in of the cell membrane is shown in Fig. 6D where well-separated DC-SIGN domains are clearly visible. The line traces through two different clusters in Figs. 6E and 6F demonstrate the superior resolution of NSOM with respect to the diffraction-limited resolution of confocal microscopy. The FWHM of a Gaussian fit to the fluorescence profiles render values of 90 and 120 nm for the line traces shown in Figs. 6E and 6F, respectively. The difference in intensity (9×10^4 and 1.6×10^5 counts/s for 6E and 6F, respectively) indicates that a different number of proteins are involved in both domains. Thus, clustering of DC-SIGN is also apparent in these images, consistent with our previous observations using TEM *(7)* and NSOM *(31)* on dried DCs, and confirming that, indeed, DC-SIGN is organized into subdiffraction-limit-sized domains in the membrane of immature DCs.

Conclusions and Outlook

In this article we have provided examples of the applicability of near-field scanning optical microscopy for studying the heterogeneity and lateral organization of the cell membrane on both dried and liquid conditions. NSOM combines the high resolution of scanning probe microscopy with the contrast of optical microscopy. Single molecule detection sensitivity combined with high-spatial resolution allows quantitative differentiation between monomer vs clustered type of organization. Furthermore, the small excitation volume of NSOM allows independent observation of individual molecules at physiological relevant packing densities, which is more than one order of magnitude higher than achieved by confocal or wide field imaging *(36)*.

Until recently, technical difficulties when operating NSOM in liquid conditions have restricted its use to fixed, dried cells, hampering its broad applicability in the biological community. We have now demonstrated that NSOM can be reliably operated in physiological conditions using a simple concept, opening the way to high-resolution live-cell imaging. However, one must be aware that as scanning probe technique, NSOM is inherently slow, being less suitable for monitoring lateral diffusion processes of membrane complexes. On the other hand, its excellent axial resolution should allow for the monitoring of exo- and endocytosis processes with high speed and sensitivity.

Co-localization studies, a common application of far-field fluorescence imaging in cell biology, when performed with NSOM should provide unprecedented detail and accuracy that are impossible to obtain by diffraction-limited imaging techniques. One of added advantages of illuminating via the NSOM

probe is the overlay of two or more excitation wavelengths to the same nanometric-sized excitation source, eliminating chromatic aberrations inherent to lens-based microscopy. In this context, we are currently using two-color excitation NSOM in liquid conditions to investigate the association of specific membrane proteins to lipid rafts. Until now, possible association between lipid rafts and proteins have been studied using biochemical methods in combination with confocal techniques based on co-patching *(37)*. In the years to come, NSOM will certainly become an important nanotool in cell biology, contributing to the understanding of the current model for the micro- and nano-scale organization of the cellular plasma membrane.

Acknowledgments

We are grateful to J. Korterik, F. B. Segerink, and B. Joosten for technical support and fruitful discussions. The research of B.I.dB. has been made possible by a grant from the Technology Foundation (STW) of the Netherlands. F.dL. and M.K. are supported by the Netherlands Foundation for Fundamental Research of Matter (FOM). A.C. is supported by the Netherlands Organization of Scientific Research, Earth and Life Sciences (SLW).

References

1. Yechiel, E. and Edidin, M. (1987), *J. Cell. Biol.* **105,** 755–760.
2. Jacobson, K., Sheets, E. D., and Simson, R. (1995), *Science* **268,** 1441–1442.
3. Kusumi, A. and Sako, Y. (1996), *Curr. Opin. Cell Biol.* **8,** 566–574.
4. Simons, K. and Ikonen, E. (1997), *Nature* **387,** 569–572.
5. Simons, K. and Toomre, D. (2000), *Nat. Rev. Mol. Cell Biol.* **1,** 31–39.
6. Vereb, G., Szollosi, J., Matko, J., et al. (2003), *Proc. Nat. Acad. Sci. USA* **100,** 8053–8057.
7. Cambi, A., de Lange, F., van Maarseveen, N.M., et al. (2004), *J. Cell Biol.* **164,** 145–155.
8. Krishnan, R. V., Varma, R., and Mayor, S. (2001), *J. Fluorescence* **11,** 211–226.
9. Sharma, P., Varma, R., Sarasij, R. C., et al. (2004), *Cell* **116,** 577–589.
10. Subczynski, W. K. and Kusumi, A. (2003), *Biochim. Biophys. Acta* **1610,** 231–243.
11. Stephens, D. J. and Allan, V. J. (2003), *Science* **300,** 82–86.
12. Michalet, X., Kapanidis, A. N., Laurence, T., et al. (2003), *Annu. Rev. Biophys. Biomol. Struct.* **32,** 161–182.
13. Betzig, E. and Chichester, R. J. (1993), *Science* **262,** 1422–1425.
14. Moerner, W. E. and Orrit, M. (1999), *Science* **283,** 1670–1676.
15. Moerner, W. E. (2002), *J. Phys. Chem. B* **106,** 910–927.
16. Tsien, R. Y. (1998), *Annu. Rev. Biochem.* **67,** 509–544.
17. Lippincott-Schwartz, J. and Patterson, G. H. (2003), *Science* **300,** 87.
18. Sako, Y. and Yanagida, T. (2003), *Nat. Cell Biol.* Suppl. S, SS1.
19. Hell, S. W. and Stelzer, E. H. (1992), *J. Opt. Soc. Am.* **9,** 2159–2166.
20. Klar, T. A., Jakobs, S., Dyba, M., Egner, A., and Hell, S. W. (2000), *Proc. Natl. Acad. Sci. USA* **97,** 8206–8210.
21. Jares-Erijman, E. A. and Jovin, T. M. (2003), *Nat. Biotech.* **21,** 1387–1395.
22. Betzig, E. and Trautman, J. K. (1992), *Science* **257,** 189.
23. Paesler, M. A. and Moyer, P. J. (1996), *Near-Field Optics, Theory, Instrumentation and Applications,* Wiley-Interscience, Network.
24. de Lange, F., Cambi, A., Huijbens, R., et al. (2001), *J. Cell Sci.* **114,** 4153–4160.
25. Laurence, T. A. and Weiss, S. (2003), *Science* **299,** 667.
26. van Hulst, N. F., García-Parajó, M. F., Moers, M. H. P., Veerman, J. A., and Ruiter, A. G. T. (1997), *J. Struct. Biol.* **119,** 222–228.
27. Enderle, Th., Ha, T., Ogletree, D. F., Chemla, D. S., Magowan, C. and Weiss S. (1997), *Proc. Natl. Acad. Sci. USA* **94,** 520–525.
28. Nagy, P., Matyus, L., Jenei, A., et al. (2001), *J. Cell Sci.* **114,** 4153.
29. Hwang, J., Gheber, L. A., Margolis, L., and Edidin, M. (1998), *Biophys. J.* **74,** 2184–2190.
30. Ianoul, A., Street, M., Grant, D., Pezacki, J., Taylor, R., and Johnston, L. J. (2004), *Biophys. J.* **87,** 3525–3535.
31. de Bakker, B. I., de Lange, F., Cambi, A., et al. (2004), submitted.
32. Koopman, M., Cambi, A., de Bakker, B. I., et al. (2004), *FEBS Lett.* **573,** 6–10.
33. Veerman, J. A., Otter, A. M., Kuipers, L., and van Hulst, N. F. (1998), *Appl. Phys. Lett.* **72,** 3115–3117.
34. Koopman, M., de Bakker, B. I., García-Parajó, M. F., and van Hulst, N. F. (2003), *Appl. Phys. Lett.* **83,** 5083–5085.
35. Ris, H. (1985), *J. Cell Biol.* **100,** 1474.
36. Vrljic, M., Nishimura, S. Y., Brasselet, S., Moerner, W. E., and McConnell, H. M. (2002), *Biophys. J.* **83,** 2681.
37. Fra, A. M., Williamson, E., Simons, K., and Parton, R. G. (1994), *J. Biol. Chem.* **269,** 30745.